

Journal of Visualized Experiments

Systems analysis of the neuroinflammatory and hemodynamic response to traumatic brain injury --Manuscript Draft--

Article Type:	Invited Methods Collection - JoVE Produced Video
Manuscript Number:	JoVE61504R2
Full Title:	Systems analysis of the neuroinflammatory and hemodynamic response to traumatic brain injury
Keywords:	Mild traumatic brain injury; cerebral blood flow; Neuroinflammation; multiplexed ELISA; partial least squares regression; cytokines; phospho-proteins
Corresponding Author:	Rowan Brothers Emory University Atlanta, Georgia UNITED STATES
Corresponding Author's Institution:	Emory University
Corresponding Author E-Mail:	robroth@emory.edu
Order of Authors:	Rowan Brothers Sara Bitarafan Alyssa Pybus Levi B. Wood Erin M. Buckley
Additional Information:	
Question	Response
Please indicate whether this article will be Standard Access or Open Access.	Standard Access (US\$2,400)
Please indicate the city, state/province, and country where this article will be filmed . Please do not use abbreviations.	Atlanta, GA, USA

TITLE:

Systems Analysis of the Neuroinflammatory and Hemodynamic Response to Traumatic Brain Injury

AUTHORS AND AFFILIATIONS:

Rowan O. Brothers^{1,*}, Sara Bitarafan^{2,3,*}, Alyssa F. Pybus^{1,3}, Levi B. Wood^{1,2,3,¥,^}, Erin M. Buckley^{1,4,5,¥,^}

¹Wallace H. Coulter Department of Biomedical Engineering, Georgia Institute of Technology and Emory University, USA

²George W. Woodruff School of Mechanical Engineering, Georgia Institute of Technology, USA

³Parker H. Petit Institute for Bioengineering and Bioscience, Georgia Institute of Technology, USA

⁴Department of Pediatrics, Emory University School of Medicine, USA

⁵Children's Healthcare of Atlanta, Children's Research Scholar, USA

*These authors contributed equally.

^Corresponding author.

¥Equally contributing senior authors

Email addresses of co-authors:

Rowan O. Brothers (robroyth@emory.edu)

Sara Bitarafan (sbitarafan74@gatech.edu)

Alyssa F. Pybus (afpybus@gatech.edu)

Corresponding authors:

Erin M. Buckley (erin.buckley@emory.edu)

Levi B. Wood (levi.wood@me.gatech.edu)

KEYWORDS:

Mild traumatic brain injury, cerebral blood flow, neuroinflammation, multiplexed ELISA, partial least squares regression, cytokines, phospho-proteins

SUMMARY:

This protocol presents methods to characterize the neuroinflammatory and hemodynamic response to mild traumatic brain injury and to integrate these data as part of a multivariate systems analysis using partial least squares regression.

ABSTRACT:

Mild traumatic brain injuries (mTBIs) are a significant public health problem. Repeated exposure to mTBI can lead to cumulative, long-lasting functional deficits. Numerous studies by our group and others have shown that mTBI stimulates cytokine expression and activates microglia, decreases cerebral blood flow and metabolism, and impairs cerebrovascular reactivity. Moreover, several works have reported an association between derangements in these neuroinflammatory and hemodynamic markers and cognitive impairments. Herein we detail methods to characterize the neuroinflammatory and hemodynamic tissue response to

mTBI in mice. Specifically, we describe how to perform a weight-drop model of mild traumatic brain injury, how to longitudinally measure cerebral blood flow using a non-invasive optical technique called diffuse correlation spectroscopy, and how to perform a Luminex multiplexed immunoassay on brain tissue samples to quantify cytokines and immunomodulatory phosphoproteins (e.g., within the MAPK and NFκB pathways) that respond to and regulate activity of microglia and other neural immune cells. Finally, we detail how to integrate these data using a multivariate systems analysis approach to understand the relationships between all these variables. Understanding the relationships between these physiologic and molecular variables will ultimately enable us to identify mechanisms responsible for mTBI.

INTRODUCTION:

Overview

Mild traumatic brain injuries (mTBIs) impact ~1.6-3.8 million athletes annually¹. These injuries, including sub-concussive and concussive injuries, can leave patients with transient physical, emotional, psychological and cognitive symptoms². Moreover, *repetitive* mTBI (rmTBI) sustained within a “window of vulnerability” can lead to cumulative severity and duration of cognitive consequences that last longer than the effects of a single mTBI alone³, and ultimately even to permanent loss of function⁴⁻⁶. Although many patients recover within a relatively short time frame (<1 week), 10-40% of patients suffer longer lasting effects of mTBI for > 1 month, with some lasting up to 1 year^{3,7-9}. Despite the high prevalence and lasting consequences of these injuries, injury mechanisms are poorly understood and no effective treatment strategies exist.

Given the high variability in outcomes after mTBI/rmTBI, one challenge in identifying early-stage molecular triggers from tissue obtained in terminal mTBI/rmTBI studies is the lack of longitudinal data demonstrating definitive acute links to longer-term outcomes. To overcome this challenge, our group has discovered that acutely reduced cerebral blood flow strongly correlates with longer-term cognitive outcomes in a mouse model of rmTBI¹⁰. Using this hemodynamic biomarker, we showed that mice with acutely low cerebral blood flow (and, by extension, worse predicted long-term outcome) have concomitant acute increases in neuronal phospho-signaling within both MAPK and NFκB pathways, increases in neuronal expression of pro-inflammatory cytokines, and increases in expression of the phagocyte/microglial marker Iba1¹¹. These data suggest a possible role for neuronal phospho-signaling, cytokine expression, and microglial activation in both the acute regulation of cerebral blood flow post injury as well as in triggering a signaling cascade that leads to neuronal dysfunction and worse cognitive outcome. Herein, we detail an approach to simultaneously probe both the hemodynamic and neuroinflammatory environment after rmTBI and how to integrate these complex datasets. Specifically, we outline procedures for four key steps to this comprehensive approach: (1) a weight-drop model of mild traumatic brain injury, (2) assessment of cerebral blood flow with diffuse correlation spectroscopy, (3) quantification of the neuroinflammatory environment, and (4) data integration (**Figure 1**). Below, we provide a brief introduction to each of these key steps to help guide readers through the rationale behind the methods. The remainder of the manuscript provides a detailed protocol for each of these key steps.

Weight-drop model of mild traumatic brain injury

Although many excellent preclinical models of repetitive mild TBI exist^{12–18}, we employ a well-established and clinically relevant weight-drop closed head injury model. Key features of this model include (1) blunt impact of the intact skull/scalp followed by unrestricted rotation of the head about the neck, (2) no overt structural brain injury, edema, blood–brain barrier damage, acute cell death, or chronic brain tissue loss, and (3) persistent (up to 1 year) cognitive deficits that emerge only after multiple hits¹⁹ (**Figure 2**).

Assessment of cerebral blood flow with diffuse correlation spectroscopy

Diffuse correlation spectroscopy (DCS) is a noninvasive optical technique that measures blood flow^{5,20,21}. In DCS, a near-infrared light source is placed on the tissue surface. A detector is placed at a fixed distance from the source on the tissue surface to detect light that has multiply scattered through the tissue (**Figure 3**). Scattering off moving red blood cells causes the detected light intensity to fluctuate with time. A simple analytical model known as correlation diffusion theory is used to relate these intensity fluctuations to an index of blood flow (CBF_i, **Figure 4**). Although the units of CBF_i (cm²/s) are not the traditional units of flow (mL/min/100 g), a previous study in mice has shown that CBF_i strongly correlates with cerebral blood flow measured by arterial spin labeled MRI²¹.

For reference, the DCS instrument used here was built in-house and is comprised of an 852 nm long coherence-length laser, an array of 4 photon counting avalanche photodiodes, and a hardware autocorrelator board (single tau, 8 channel, 100 ns minimum sample time)^{21,22}. Data is acquired with homemade software written in LabView. The animal interface for the device consists of a 3 m long 400 μm multimode source fiber (400–2200 nm wavelength range, pure silica core, TECS Hard Cladding) and a 3 m long 780 nm single mode detector fiber (780–970 nm wavelength range, pure silica core, TECS Hard Cladding, 730 ± 30 nm second mode cut-off) spaced 6 mm apart and embedded in a black 3D-printed sensor (4 mm x 8 mm, **Figure 3**).

Quantification of the neuroinflammatory environment

Although neuroinflammation is regulated by diverse cellular processes, two key relevant mechanisms are extracellular signaling by cytokines/chemokines and intracellular signaling by phospho-proteins. To investigate the neuroinflammatory environment of the brain post-injury, brains are extracted from mice, microdissected, and cytokines/chemokines and phospho-proteins are quantified using Luminex (**Figure 5, 6**). Luminex multiplexed immunoassays enable simultaneous quantification of a diverse collection of these proteins by coupling enzyme-linked immunosorbent assays (ELISAs) to fluorescently tagged magnetic beads. Distinct fluorescent tags are used for each protein of interest, and beads of each tag are functionalized with a capture antibody against that particular protein. Hundreds of beads for capturing each protein are mixed together, placed in a 96 well plate, and incubated with sample. After sample incubation, a magnet is used to trap the beads in the well while the sample is washed out. Next, biotinylated detection antibody binds to the analyte of interest to form an antibody-antigen sandwich similar to a traditional ELISA, but with the ELISA for each protein occurring on a different fluorescently tagged bead. Adding phycoerythrin-conjugated streptavidin (SAPE)

completes each reaction. The Luminex instrument then reads the beads and separates the signal according to each fluorescent tag/protein.

Data integration

Because of the large number of analytes (e.g., cytokines) measured in the Luminex assay, data analysis can be difficult to interpret if each quantified protein is analyzed individually. To simplify analysis and to capture trends observed among analytes, we use a multivariate analysis method called partial least squares regression (PLSR, **Figure 7**)²³. PLSR works by identifying an axis of weights corresponding to each measured protein (i.e., cytokines, phospho-proteins, referred to as “predictor variables”) that together optimally explain co-variance of the measured proteins with a response variable (e.g., cerebral blood flow). The weights are referred to as “loadings” and are assembled into a vector known as a latent variable (LV). By projecting (referred to as “scoring”) the measured protein data on each of two LVs, the data can be re-plotted in terms of these LVs. After computing the PLSR, we use a varimax rotation to identify a new LV that maximizes the covariance between the sample projections onto the LV and the predictor variable²⁴. This approach allows us to define LV1 as the axis for which the variance of the response variable is best explained. LV2 maximizes co-variance between the response variable and LV1 residual data, which may be associated with biological or technical variability between samples. Lastly, we conduct a Leave One Out Cross Validation (LOOCV) to ensure that the PLSR model is not heavily dependent upon any one sample²³.

In this protocol, we detail methods to characterize the neuroinflammatory and hemodynamic tissue response to mTBI. The general workflow is outlined in **Figure 1**. In this protocol, mice are subject to one or more mTBIs using a weight-drop closed head injury model. Cerebral blood flow is measured longitudinally before and at multiple time points after injury. At the time point of interest for interrogation of neuroinflammatory changes, the animal is euthanized, and the brain is extracted. Brain regions of interest are isolated via microdissection and then lysed to extract protein. Lysates are then used for both Luminex multiplexed immunoassays of cytokine and phospho-protein expression as well as Western blot. Finally, this holistic dataset is integrated using a partial least squares regression analysis.

PROTOCOL:

All animal procedures are approved by Emory University Institutional Animal Care and Use Committee (IACUC) and followed the NIH Guidelines for the care and Use of Laboratory Animals.

1. Weight-drop model of mild traumatic brain injury

1.1. Prepare the weight-drop setup. Mount a vise on a flat surface with a 1 m guide tube (2.54 cm inner diameter) aligned vertically (check using a level). Use a 54 g bolt (0.95 cm basic body diameter, 2 cm head diameter, 10.2 cm length) for the impact.

1.2. Briefly anesthetize mouse. Induce the mouse with 4.5% isoflurane in 100% oxygen for 45

seconds. Confirm sufficient depth of anesthesia by the lack of a toe pinch response.

1.3. Induce injury.

1.3.1. Rapidly remove the mouse from anesthesia and place the mouse prone on the center of a thin membrane (11.2 cm x 21.3 cm tissue).

1.3.2. Use both hands to hold the tissue taut with the mouse prone on the center. Secure the mouse's tail under a thumb. Position the mouse head under the guide tube (**Figure 2**).

1.3.3. Drop the bolt from the top of the guide tube onto the dorsal aspect of the mouse's head, aiming for impact between the back of the eyes and the front of the ears. Upon impact, the mouse will penetrate the tissue, allowing for rapid acceleration of the head about the neck (**Figure 2**).

1.4. Recovery

1.4.1. After impact, place the mouse supine on a 37 °C warming pad in room air. Monitor recovery for 1 h post-injury. Within 1 h, mice should be able to ambulate normally, find food and water, and not exhibit gross motor deficits.

NOTE: Loss of consciousness, defined as the time from removal from anesthesia to the time to regain righting reflex, is expected and typically lasts from 20 s to 3 minutes (**Supplemental Table 1**). Brief (<30 s) episodes of apnea and/or seizure-like activity may be observed, particularly after repetitive head injuries spaced once-daily.

1.5. Repeat as needed. This injury may be repeated once-daily, weekly, or monthly. The number and spacing of injuries depend on desired injury severity. Typically, we employ five hits spaced once daily to induce robust deficits in spatial learning and memory.

2. Assessment of cerebral blood flow with diffuse correlation spectroscopy

2.1. DCS data acquisition

2.1.1. Remove hair on the scalp. Because DCS works best in the absence of hair, it is necessary to remove fur on the head prior to the start of experiments. Typically, hair removal is done 1-3 days prior to the start of the study.

2.1.1.1. Induce mice with 4.5% isoflurane in 100% oxygen for 45 seconds and maintain with 1-2% isoflurane in 100% oxygen.

2.1.1.2. Shave the head between the eyes and the ears. Then, use depilatory cream to remove fur on the head as in **Figure 3**.

2.1.1.3. Allow the animal to recover from anesthesia on a warming pad and then return to cage.

2.1.2. Measure cerebral blood flow with DCS. To minimize motion artifacts during measurement, study mice under brief isoflurane anesthesia.

NOTE: Visually monitor respiration and toe pinch response throughout measurements and adjust isoflurane concentration as needed to ensure consistent depth of anesthesia. Significant variations in the depth of anesthesia could alter blood flow given the known vasomodulatory effects of isoflurane²⁵.

2.1.2.1. Induce with 4.5% isoflurane in 100% oxygen for 45 seconds, and then maintain with 1.0-1.75% isoflurane in 100% oxygen. Confirm sufficient depth of anesthesia by the absence of a toe pinch response and normal respiration (between ~60-80 breaths per minute).

2.1.2.2. After a 2 min period of stabilization, gently rest the DCS sensor over the right hemisphere such that the top edge of the optical sensor lines up with the back of the eye and the side of the sensor lines up along the midline (**Figure 3**). Cup a hand over the sensor to shield from room light. Acquire 5 seconds of data (1 Hz acquisition).

2.1.2.3. Reposition the sensor over the left hemisphere, and acquire 5 seconds of data.

2.1.2.4. Repeat 3 times/hemisphere to account for local heterogeneities under the tissue surface.

2.1.3. Recovery

2.1.3.1. Remove the mouse from anesthesia and place on a warming pad.

2.1.3.2. After the mouse regains its righting reflex return it to the cage.

2.2. DCS data analysis

2.2.1. Perform initial quality control. Each frame of DCS data consists of a measured normalized intensity autocorrelation function, $g_2(\tau)$ (**Figure 4A**), and photon count rate (kHz).

2.2.1.1. To remove data frames with significant motion artifact, discard data frames for which the mean value of the tail of the $g_2(\tau)$ curve (i.e., $g_2(\tau > .018 \text{ s})$) is > 1.005 .

2.2.1.2. To remove data frames with poor signal-to-noise ratio, discard data frames if the detected photon count rate is $< 20 \text{ kHz}$.

2.2.2. Extract cerebral blood flow index. Using *fminsearch* in Matlab, fit each i^{th} measured data frame ($g_{2,meas\ i}(\tau)$) for $\text{CBF}_i(i)$. Restrict fits to $g_{2,meas\ i}(\tau) > 1.05$, and find the value of CBF_i that

minimizes the following cost function:

$$\chi^2 = \sum_j \left(g_{2,meas}(\tau_j) - g_{2,fit}(\tau_j) \right)^2, \quad (1)$$

Where the sum is over all measured delay times, τ_j , and $g_{2,fit}(\tau)$ is the semi-infinite homogeneous solution of the correlation diffusion equation (**Figure 4B**):

$$g_{2,fit}(\tau) = 1 + \beta \left(\frac{\frac{e^{-K(\tau)r_1}}{r_1} - \frac{e^{-K(\tau)r_2}}{r_2}}{\frac{e^{-K(0)r_1}}{r_1} - \frac{e^{-K(0)r_2}}{r_2}} \right)^2. \quad (2)$$

Here β is a coherence factor determined by the experimental set up, $K(\tau) = \sqrt{(3\mu_a\mu'_s + 6\mu'_s k_0^2 \tau \text{CBF}_i)}$, $r_1 = \sqrt{\rho^2 + z_0^2}$, $r_2 = \sqrt{\rho^2 + (z_0 + 2z_b)^2}$, $z_0 = 1/\mu'_s$, $z_b = 2(1 + R_{eff})/3\mu'_s(1 - R_{eff})$, $R_{eff} = 0.493$ for an assumed tissue index of refraction of 1.4, ρ is 6 mm, and μ_a and μ'_s are the absorption and reduced scattering coefficient of the tissue (assumed to be 0.25 and 9.4/cm, respectively^{10, 26, 27}).

NOTE: Because β can vary ~10% over time, fit each data frame for β and CBF_i simultaneously.

2.2.3. Perform secondary quality control. Within each repetition (which consists of 5 data frames), discard outliers. Outliers are defined as those CBF_i values that fall outside 1.5 standard deviations of the mean CBF_i for that repetition. If more than 1 data point is identified as an outlier, discard the entire repetition.

2.2.4. Estimate average cerebral blood flow index: Estimate an average CBF_i per hemisphere by taking the mean across all data frames for all repetitions (**Figure 4C**). If no significant hemispheric differences are observed, average across hemispheres to obtain an estimate of average global CBF_i .

3. Multiplexed quantification of cytokines and phospho-proteins using luminex assays

3.1. Tissue extraction

NOTE: Quantification of brain cytokines and phospho-signaling proteins using Luminex requires tissue extraction.

3.1.1. Anesthetize mouse using 4.5% isoflurane in 100% oxygen for 1-2 min. Check for deep plane of anesthesia via the lack of a toe pinch response. Euthanize via decapitation.

3.1.2. Harvest the tissue.

3.1.2.1. Remove the brain. Typically, fix the left hemisphere for histology and microdissect several regions from the right hemisphere within the cortex and hippocampus (**Figure 5**).

3.1.2.2. Place dissected samples in microcentrifuge tubes, flash freeze in liquid nitrogen. For analysis of freeze-sensitive proteins, it is optimal to sub-divide tissue sections prior to flash freezing to avoid later freeze-thaw.

NOTE: The protocol can be paused, and tissue samples can be stored at -80 °C until ready to lyse samples. Alternatively, samples can be lysed, and then stored at -80 °C.

3.1.3. Lyse samples.

3.1.3.1. Prepare the lysis buffer by adding protease inhibitor and 2 mM phenylmethylsulfonyl fluoride to the lysis buffer.

3.1.3.2. Add 150 µL of the mixed lysis buffer per approximately 3 µg of animal tissue. For reference, mouse visual cortex tissue samples are approximately 3 µg.

3.1.3.3. To homogenize the tissue, mechanically triturate the tissue by pipetting up and down ~15-20 times using a 1000 µL pipette. For optimal sample trituration, a homogenizer pestle can be used.

3.1.3.4. Place the sample tubes on a rotator for 30 min at 4 °C.

3.1.3.5. Centrifuge the samples at 4 °C for 10 min at approximately 15,000 x *g*, and collect the supernatant. Samples may be processed immediately or stored at -80 °C for further analysis.

NOTE: Sample lysates prepared using this protocol are compatible with Western blot, from which the phagocyte/microglial marker Iba1 and/or the astrocyte activation marker GFAP can be analyzed to complement cytokine and phospho-protein analysis for neuroinflammation studies¹¹.

3.2. Multiplex immuno-assay protocol for cytokines and phospho-proteins

NOTE: Although similar overall, there are some minor differences in the protocols for cytokine and phospho-protein kits. Differences are noted in each step. The steps to prepare samples for the Luminex assay are outlined below.

3.2.1. Preparation of reagents (day 1, same for cytokine and phospho-proteins)

3.2.1.1. Allow reagents to warm to room temperature (~30 min).

3.2.1.2. Sonicate multiplex magnetic beads bottle for 30 seconds followed by 1 min of vortexing. Ensure multiplex magnetic beads are shielded from light with aluminum foil or use provided light protective bottles.

3.2.1.3. Prepare wash buffer by mixing 0.1% Tween20 in 1xPBS or alternatively use the wash buffer provided in the kit.

3.2.2. Preparation of lysed tissue samples (day 1, same for cytokine and phospho-protein)

3.2.2.1. If previously frozen, remove lysed tissues samples from freezer and allow to thaw on ice (~20 min). Centrifuge samples for 10 min at 9,167 x g to remove precipitate.

3.2.2.2. Prepare 25 µL of sample at the optimal protein concentration determined by the linear range analysis (see section 3.3). To normalize total volume for all samples, dilute samples in assay buffer provided in the kit.

3.2.3. Preparation of 96 well plate (day 1, same for cytokine and phospho-proteins)

3.2.3.1. Use the 96 well plate included in the kit or one with a thin bottom (e.g., Brand Tech).

3.2.3.2. Add 200 µL of wash buffer (or 1x PBS, 0.1% Tween) into each well and mix on plate shaker for 10 min at 750 rpm.

3.2.3.3. Decant wash buffer and tap the plate onto a paper towel to remove residue.

3.2.4. Immunoassay procedure for Cytokines (day 1)

3.2.4.1. Add the following to each well in order.

3.2.4.1.1. Add 25 µL of assay buffer to all wells.

3.2.4.1.2. Add 25 µL of additional assay buffer ONLY to background wells. For every experimental run, have at least two background wells. Background wells have no sample loaded and define the fluorescent intensity read by the instrument without sample.

3.2.4.1.3. Add 25 µL of diluted samples to samples wells.

3.2.4.1.4. Add 25 µL of 1x multiplex magnetic beads to all wells (**Figure 6**). Be sure to vortex beads for 1 min before adding to wells.

3.2.4.2. Seal plate with plate sealer and cover the plate with aluminum foil. Incubate overnight (12-16 h) at 2-8 °C.

3.2.5. Immunoassay procedure for cytokines (day 2)

3.2.5.1. Place 96 well plate on magnetic separator, making sure that the wells are aligned with the magnets. Let sit for 2 min. Decant well contents while the plate is still attached to the magnetic separator.

3.2.5.2. Wash plate 2 times using the following steps.

3.2.5.2.1. Add 200 μ L of wash buffer and place on shaker for 2 min at room temperature.

3.2.5.2.2. Place the well plate on the magnetic separator for 2 min at room temperature.

3.2.5.2.3. Decant well contents while the well plate is still attached to magnetic separator.

3.2.5.3. Add 25 μ L of detection antibody per well (**Figure 6**). Cover with foil. Incubate for 1 hour on a plate shaker (750 rpm) at room temperature.

3.2.5.4. Leave the detection antibody in and add 25 μ L of streptavidin-phycoerythrin (SAPE) (**Figure 6**). Cover with foil. Incubate for 30 min on plate shaker (750 rpm) at room temperature.

3.2.5.5. Place the well plate on a magnetic separator and let sit for 2 min. Decant well contents and detach from magnetic separator.

3.2.5.6. Wash well plate two times (see step 3.2.5.2).

3.2.5.7. Add 75 μ L of Luminex Drive Fluid (if using MAGPIX instrument) or assay buffer (if using 200 or FlexMap 3D instrument). Re-suspend beads on plate shaker for 5 min at room temperature.

3.2.5.8. Read on Luminex Instrument (MAGPIX, 200, or FlexMap 3D), referring to the user's manual for proper operation (**Figure 6**).

3.2.6. Immunoassay procedure for phospho-proteins (day 1)

3.2.6.1. Add the following to each well in order.

3.2.6.1. Add 25 μ L of assay buffer to all wells.

3.2.6.1.1 Add 25 μ L of additional assay buffer ONLY to background wells. For every experimental run, it is recommended to have at least two background wells. Background wells have no sample loaded and define the fluorescent intensity read by the instrument without sample.

3.2.6.1.2 Add 25 μ L of diluted samples to samples wells.

3.2.6.1.3 Add 25 μ L of 1x multiplex magnetic beads to all wells (**Figure 6**).

NOTE: The Luminex assay kit provides multiplex magnetic bead in 20x stock solution. Be sure to vortex 20x stock multiplex magnetic bead solution for 2 min, and then dilute it in assay buffer to 1x solution. Vortex 1x multiplex magnetic bead suspension for 1 min before adding to wells.

3.2.6.2 Seal plate with plate sealer and cover the plate with aluminum foil. Incubate overnight

(12-16 hours) at 2-8 °C.

3.2.7. Immunoassay procedure for phospho-protein (day 2)

3.2.7.1. Place the well plate on a magnetic separator, making sure that the well plate is fully aligned with the magnetic separator. Let sit for 2 min. Decant well contents while the well plate is still attached to the magnetic separator.

3.2.7.2. Wash plate 2 times (see step b in cytokine's immunoassay procedure day 2).

3.2.7.3. Dilute the 20x stock detection antibody to 1x solution in assay buffer. Add 25 µL of 1x detection antibody per well (**Figure 6**). Cover with foil. Incubate for 1 h on plate shaker (750 rpm) at room temperature.

3.2.7.4. Place the 96 well plate on magnetic separator, and let sit for 2 min. Decant well contents, detach from the magnetic separator

3.2.7.5. Dilute 25x stock streptavidin-phycoerythrin (SAPE) in assay buffer to 1x buffer. Add 25 µL of 1x SAPE (**Figure 6**). Cover with foil and incubate for 15 min on plate shaker (750 rpm) at room temperature.

3.2.7.6. Leave the SAPE in wells, and add 25 µL of amplification buffer to each well. Cover with foil. Incubate for 15 min on plate shaker (750 rpm) at room temperature.

3.2.7.7. Incubate for 15 min on plate shaker (750 rpm) at room temperature.

3.2.7.8. Place the well plate on the magnetic separator for 2 min. Decant well contents and detach from the magnetic separator.

3.2.7.9. Add 75 µL of Luminex Drive Fluid (if using MAGPIX instrument) or assay buffer (if using 200 or FlexMap 3D instrument). Re-suspend beads on a plate shaker for 5 min at room temperature.

3.2.7.10. Read on Luminex instrument (MAGPIX, 200, or FlexMap 3D), referring to the user's manual for proper operation (**Figure 6**).

3.3. Linearity of sample dilution curve

3.3.1. Preparation of samples: Serially dilute test samples with different concentration of total protein. For bulk brain tissues, load serial dilutions from 0-25 µg for cytokines and 0-12 µg for phospho-proteins. Total protein concentration can be measured using bicinchoninic acid (BCA) assay.

3.3.2. Multiplex immunoassay: Perform the Luminex assay (see section 3.2) on selected samples.

3.3.3. Data analysis

3.3.3.1. Plot fluorescent intensity for each protein vs. amount of protein loaded (**Figure 7**).

3.3.3.2. For each analyte, identify range of total protein loaded for which the relationship between total protein and the fluorescent intensity readout is linear (**Figure 7**).

3.3.3.3. To determine the amount of total protein that should be loaded for the full assay run, identify the linear portion of the curve for each analyte and then select a protein concentration that falls within the linear range for the majority of analytes.

NOTE: Although most proteins share a similar linear range, the linear ranges may not overlap for all proteins. If this is the case, it may be necessary to run each sample multiple times with different amounts of total protein loaded. Alternatively, nonlinear samples may be left out of the analysis. Additionally, some proteins may not have a linear range whatsoever.

4. Partial least squares regression

NOTE: Sample R code and a sample data spreadsheet are provided to carry out the Partial Least Squares Analysis.

4.1. Data Preparation: Format the data as shown in the provided sample data spreadsheet, "MyData". Include variable names in the row 1, sample names in column A, the response variable in column B, and all predictor variables in columns C+. Fill the last two rows with the background data, and set both sample names to "Background".

4.2. Partial Least Squares Regression in RStudio

4.2.1. Install R from www.r-project.org (free, open source).

4.2.2. Install RStudio Desktop from www.rstudio.com (free, open source license).

4.2.3. Download the sample R code provided with this publication, "PLSR_Sample_Code.R" and save it to the same folder which contains the data spreadsheet. Open the code file in RStudio.

4.2.4. In the **User Input** section, change "dataFileName" to the name of the data spreadsheet.

4.2.5. Carry out the following steps by highlighting the section of code to run and clicking **Run** in the top right corner of the script.

4.2.5.1. Load necessary R packages, functions, the working directory address, and user

input values in RStudio (subsection “Preliminaries”).

4.2.5.2. Load the data into RStudio and prepare raw data for processing by subtracting mean background signal from all measurements and z-scoring each analyte (subsection “Read Data and Subtract Background”)(**Figure 8A**).

4.2.5.3. Perform partial least squares regression in RStudio using the plsRglm package v1.2.5²⁸ available on the Comprehensive R Archive Network (CRAN). Perform a varimax rotation (stats package v3.6.2)²³ in the LV1-LV2 plane to identify a new horizontal axis that best separate samples by the response variable (subsection “PLS”)(**Figure 8B**).

4.2.5.4. Conduct a Leave One Out Cross Validation (LOOCV) in which one sample is iteratively left out of the data and the PLSR model is re-computed. Compute standard deviation for analyte loadings across all LOOCV runs (subsection “LOOCV”).

4.3. Create representative plots: Run the provided sample code as detailed above to create representative plots which automatically export as pdf files to the working directory (the folder containing the data and code files).

4.3.1. Create a heat map of the processed data as shown in **Figure 8A** (subsection “PLS”). Color each entry along a spectrum defined by z-score. Sort analytes by the order computed in the latent variable of interest.

4.3.2. Create a scores plot with LV1 scores plotted along the horizontal axis and LV2 scores plotted along the vertical axis, as shown in **Figure 8B** (subsection “PLS”). Color each data point according to its response variable measurement to visualize the relationship between each latent variable and the response variable.

4.3.3. Create a bar plot displaying loadings for each of your predictor variables to visualize how each analyte contributes to the latent variables, as shown in **Figure 8C** (subsection “LOOCV”).

4.3.4. Create a plot regressing LV1 scores against your response variable to visualize how well the PLSR model separates the samples, as shown in **Figure 8D** (subsection “PLS”).

REPRESENTATIVE RESULTS:

Previously collected data were taken from prior work in which a group of eight C57BL/6 mice were subjected to three closed-head injuries (**Figure 2**) spaced once daily¹¹. In this work, cerebral blood flow was measured with diffuse correlation spectroscopy 4 h after the last injury (**Figure 3,4**). After post-injury CBF assessment, the animals were euthanized, and brain tissue was extracted for quantification of cytokines and phospho-proteins via immunoassay (**Figure 5**). We also quantified the phagocyte/microglial activation marker Iba1 via Western blot (methods described in¹¹). Brain tissue from each mouse was lysed, and total protein concentration was measured using a BCA assay. Multiplexed cytokine quantification was conducted using the Milliplex MAP Mouse Cytokine/Chemokine 32-Plex, which was read using a Luminex MAGPIX

system (**Figure 6**). A linear range analysis was conducted to determine an appropriate protein loading (12 μ g of protein per 12.5 μ L of lysate) (**Figure 8**) prior to collecting data from all samples.

Cytokine data was prepared for analysis by subtracting background measurements from sample data, and then z-scoring data for each analyte (**Figure 7A**). A heatmap was generated from z-scored data to visualize differences in cytokine expression among animals. Partial Least Squares Regression (PLSR) was conducted using the phagocyte/microglial activation marker Iba1 as the response variable and cytokine measurements as the predictor variables (**Figure 7B**). A varimax rotation was performed to maximize the co-variance of the data on LV1 with the Iba1 measurements (**Figure 7D**). High loading weights in LV1 (**Figure 7C**) correspond with the cytokine expression most associated with high expression of Iba1. Linear regressions between Iba1 and cytokines show that those cytokines with the greatest loading weights in LV1 were also statistically significant (**Figure 7E**).

Figure 1: Typical workflow. First, mice undergo a weight drop closed head injury, and then cerebral blood flow (CBF) of mice is measured using diffuse correlation spectroscopy. Next, brains are collected, regions of interest are micro-dissected and snap frozen using liquid nitrogen. In preparation for the Luminex immunoassay, proteins are lysed, and total protein concentration is measured by BCA assay. Lysates are used for Western blot of Iba1 and Luminex assays for cytokines and phospho-proteins. Data from CBF, Western blot, and Luminex are integrated using partial least squares regression (PLSR).

Figure 2: Closed-head weight drop model of mild traumatic brain injury. (A) The anesthetized mouse is grasped by the tail and placed on a taut sacrificial membrane underneath a guide tube. A 54 g weight is dropped from 1 m onto the dorsal aspect of the head. (B) Within ~1 ms post-impact, the mouse's head has rapidly rotated about the neck as it breaks through the KimWipe. (C) Within ~5 ms post-impact, the entire mouse has fallen and is hanging by its grasped tail.

Figure 3: Data acquisition with Diffuse Correlation Spectroscopy. (A) An optical sensor is gently manually held over the right hemisphere to measure blood flow in an anesthetized mouse. (B) Representative sensor placement on the right hemisphere. The outline of the sensor is represented as a dashed black rectangle, and the location of the source and detector fibers are in red and blue circles, respectively. The sensor is placed such that the short edge of the sensor lines up with the back of the eye and the long edge of the sensor aligns with the midline.

Figure 4: Diffuse Correlation Spectroscopy data analysis. (A) Representative measured intensity autocorrelation curves, $g_2(\tau)$, at baseline, pre-injury baseline (green) and 4 h after 5 closed head injuries spaced once daily (purple). The right shift in the curve from pre- to post-injury reflects a decrease in blood flow. (B) $g_2(\tau)$ data is acquired at 1 Hz for 5 s per hemisphere and repeated 3x/hemisphere. Each measured $g_2(\tau)$ curve is fit to the semi-infinite solution to the correlation diffusion equation for a cerebral blood flow index (CBFi). (C) CBF_i values across

all frames and repetitions are averaged to obtain mean cerebral blood flow index for each hemisphere.

Figure 5: Mouse brain microdissection. (A) After the brain is extracted from mouse, it is bisected along dashed line. The left hemisphere is fixed for histology, and the right hemisphere is microdissected for pathology. (B) Sagittal view of the cortex of the right hemisphere. The right hemisphere is microdissected into corresponding color-coded regions. For analysis of freeze-sensitive proteins, it is optimal to sub-divide tissue sections prior to flash freezing.

Figure 6. Illustration of Luminex procedure. (A) Add samples to fluorescently tagged beads. Beads are pre-coated with a specific capture antibody for each protein of interest. (B) Add biotinylated detection antibodies. Biotin-detection antibody will bind to the analyte of interest and form an antibody-antigen sandwich. (C) Add phycoerythrin (PE)-conjugated streptavidin (SAPE). SAPE binds to the biotinylated detection antibodies, completing the reaction. For phospho-proteins, an amplification buffer (only for phospho-protein assays) is added following the addition to SAPE to enhance the assay signal. (D) Luminex instrument (MAGPIX, 200, or FlexMap 3D) reads reaction on each fluorescently tagged bead via a combination of red/green illumination.

Figure 7: Representative Partial Least Squares Regression (PLSR) Analysis. (A) Panel cytokine protein expression (left columns) together with Iba1 expression (righthand column) in 3xCHI mice (n=8, z-scored). Cytokines annotated with a line overhead each linearly correlated with Iba1 with $p < 0.1$. (B) PLSR assigns weights (loadings) to measured cytokines for each latent variable. Weights are applied to measured data to compute scores for each sample on each latent variable. (C) PLSR of 3xCHI samples against Iba1 identified a weighted profile of cytokines, LV1, which distinguished samples by Iba1. Cytokines with negative weights were upregulated in samples with low Iba1 while cytokines with positive weights were upregulated in samples with high Iba1 (mean \pm SD using a LOOCV). (D) Linear regression of LV1 scores for each sample against Iba1. R^2_{PLS} measures the goodness of fit between Iba1 and LV1. (E) Individual regressions of Iba1 against each of the cytokines with the greatest weights in LV1 in C.

Figure 8: Illustration of sample dilution curve to identify the linear range. Protein concentration of serially diluted samples versus fluorescent intensity measured from the Luminex assay. The linear range is defined as the protein concentration range for which the relationship between the protein concentration and fluorescent intensity is linear (arrow). In some analytes, increasing the protein concentration beyond a certain limit can decrease antibody binding such that the dilution curve becomes non-linear or inverted (Hook effect).

DISCUSSION:

Herein we detail methods for assessment of the hemodynamic and neuroinflammatory response to repetitive mild traumatic brain injury. Further, we have shown how to integrate these data as part of a multivariate systems analysis using partial least squares regression. In the text below we will discuss some of the key steps and limitations associated with the protocol as well as the advantages/disadvantages of the methods over existing methods.

Weight-drop model of mild traumatic brain injury. This method of traumatic brain injury induction is advantageous in that it features blunt-impact followed by rapid anterior-posterior rotational acceleration commonly seen in sports-related head injuries^{10,19}. Certainly, the lissencephalic mouse brain does not fully recapitulate complexity of the gyrocephalic human brain; nevertheless, this model does induce many of the same clinical and behavioral sequelae of human mTBI, including sustained deficits in spatial learning and memory with repeated injuries. Additionally, while the impact is mild in nature (no structural/neuronal damage, no blood brain barrier permeability, cognitive deficits emerging only after multiple hits, etc.¹⁹), it does induce significant loss of consciousness, in contrast to humans where loss of consciousness is less common. This increased loss of consciousness may be due to an interaction with the anesthesia given immediately prior to the impact, although the exact cause is not well understood. Finally, we note that aligning the guide tube such that the bolt impacts between the coronal and lamdoid sutures is critical. We have observed that impacts that are more posterior can cause significant motor deficits that require euthanasia.

Assessment of cerebral blood flow with Diffuse Correlation Spectroscopy. Non-invasive, longitudinal measurements of cerebral blood flow (CBF) with traditional modalities used in human/large animal studies, such as perfusion magnetic resonance imaging or transcranial Doppler ultrasound, are challenging in mice for various reasons, including small brain size and total blood volume²⁹. Diffuse correlation spectroscopy is well-suited in mice and offers the added advantages of being noninvasive and relatively inexpensive compared to other modalities^{20,30}. Because DCS is sensitive to motion artifacts, mice need to be briefly anesthetized for assessment. We use isoflurane due to its fast induction and recovery; however, isoflurane is a cerebral vasodilator, and blood flow estimates under isoflurane should be interpreted with caution. Decreases in blood flow seen post-injury compared with sham-injured animals could be confounded by a failure of the injured cerebral vasculature to vasodilate in response to isoflurane. Finally, we have previously demonstrated excellent intra-user repeatability of blood flow measurements with DCS in mice but only fair intra-user repeatability²¹. For this reason, we recommend that the same operator acquire DCS measurements for experiments that require longitudinal assessment of cerebral blood flow.

Multiplexed quantification of cytokines and phospho-proteins using Luminex assays. A key challenge with any ELISA is the Hook effect, whereby increased protein concentration can reduce antibody affinity for the target protein, thus leading to decreased assay signal in response to increased protein³¹ (**Figure 8**). This effect can be exacerbated when analyzing whole tissues, wherein bulk proteins can similarly interfere. Thus, the first step in utilizing Luminex assays is to determine if there is a range of protein concentrations loaded for which the assay read out linearly varies with the amount of protein loaded. Analytes that do not have such a linear range (**Figure 8**) should be excluded from the analysis.

Because neuroinflammation is regulated by diverse intracellular phospho-proteins and extracellular cytokines, it is critical to simultaneously measure a wide array of these proteins in order to understand the brain's neural immune response to mTBI. Luminex multiplexed

immunoassays enable simultaneous quantification of dozens of cytokines and phospho-proteins from a single sample, providing a holistic view of the tissue immune response post-injury. Although these analyses provide a broad view of cytokines/chemokines as well as phospho-proteins, the assay quantifies total amount of each protein from a tissue homogenate. Thus, it does not yield cell-type specific data. However, cell-type specificity can be determined by follow-up immunohistochemistry to identify localization of top proteins of interest with markers for cell types (e.g., neurons, microglia, astrocytes, etc.)¹¹. We also note that cytokine levels in the brain are typically very low and appear near the lower detection limit assessed via standard curves supplied with the Luminex kit. For this reason, it is essential to conduct linear ranging analysis to determine if the instrument readout truly reflects the amount of sample loaded. For key proteins of interest, this linear range analysis can be complemented with a spike recovery assay wherein recombinant protein is spiked into a sample, and linearity in the instrument reading is evaluated³².

Partial least squares regression analysis for data integration. The tissue response to mTBI is multifactorial, consisting of physiological changes in blood flow together with changes in the phagocyte/microglial activation marker Iba1, diverse cytokines, and phospho-proteins, among others¹¹. Because of the multiplexed nature of the data collected, a systematic method is needed to account for the multidimensionality of the relationships between the various predictor variables. PLSR provides a suitable solution to this problem by identifying LVs that maximally identify the co-variance between the protein predictor variables and the outcome variable (e.g., Iba1 in **Figure 7**). Importantly, those proteins found to strongly correlate with the predictor variable (i.e., those with high loadings on LV1) often correlate in the univariate regression analysis as well (**Figure 7E**). Because PLSR is often used to fit a large number of predictor variables to a smaller number of samples as in **Figure 7**, it is critical to gain an understanding of the sensitivity of the weights on LV1 to individual samples. For a small number of samples (<10) LOOCV is useful for assessing the sensitivity of the weights (indicated via SD error bars in **Figure 7C**). For a larger number of samples, it will be important to assess sensitivity by leaving multiple samples out at a time using a Monte Carlo sub-sampling approach³³. We refer the reader to *Multi and Megavariate Data Analysis*²⁴ for an in-depth discussion of PLSR approaches and uses. Finally, we note that a key limitation of this type of analysis is that it is purely correlative. PLSR does not prove a mechanistic relationship between predictor variables and the outcome variable. We view PLSR as a valuable *hypothesis generating* approach that is used to suggest tractable targets to modulate in future experiments that establish causal relationships.

ACKNOWLEDGMENTS:

This project was supported by the National Institutes of Health R21 NS104801 (EMB) and Children's Healthcare of Atlanta Junior Faculty Focused Award (EMB). This work was also supported by the U.S. Department of Defense through the Congressionally Directed Medical Research Programs under Award No. W81XWH-18-1-0669 (LBW/EMB). Opinions, interpretations, conclusions and recommendations are those of the author and are not necessarily endorsed by the Department of Defense.

DISCLOSURES:

None.

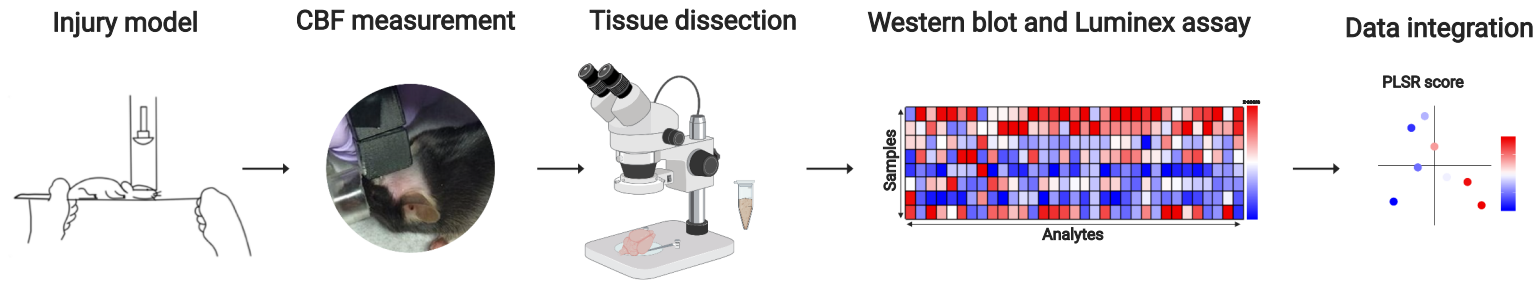
REFERENCES

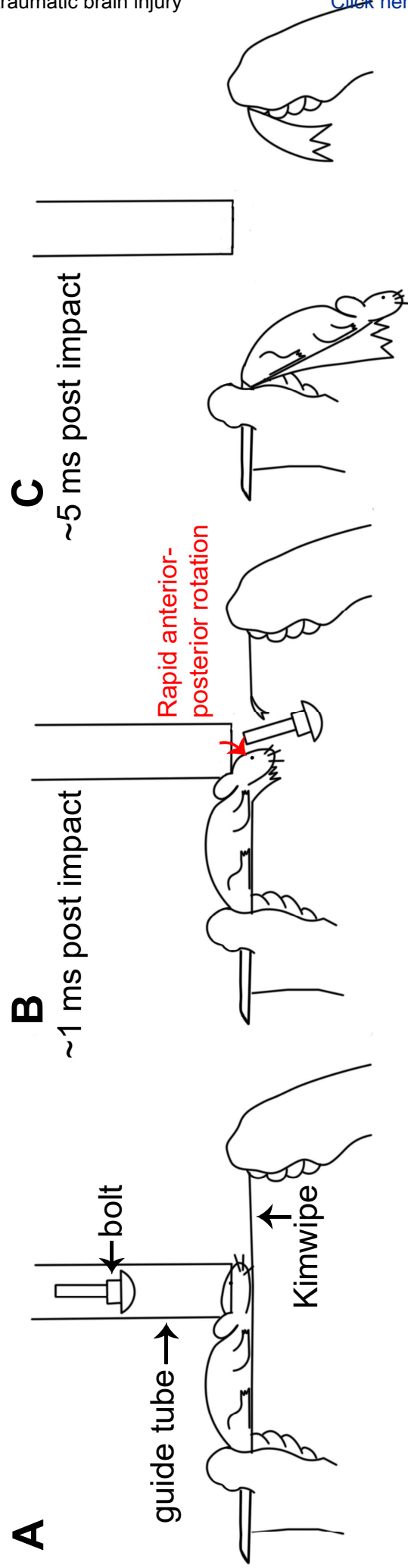
1. Langlois, J.A., Rutland-Brown, W., Wald, M.M. The epidemiology and impact of traumatic brain injury: a brief overview. *Journal of Head Trauma Rehabilitation*. **21** (5), 375–8 (2006).
2. Iraj, A. et al. Resting State Functional Connectivity in Mild Traumatic Brain Injury at the Acute Stage: Independent Component and Seed-Based Analyses. *Journal of Neurotrauma*. **32** (14), 1031–45 (2015).
3. Guskiewicz, K.M. et al. Cumulative effects associated with recurrent concussion in collegiate football players: the NCAA Concussion Study. *Journal of the American Medical Association*. **290** (19), 2549–55 (2003).
4. Longhi, L. et al. Temporal window of vulnerability to repetitive experimental concussive brain injury. *Neurosurgery*. **56** (2), 364–74 (2005).
5. Committee on Sports-Related Concussions in Youth, Board on Children, Youth, and Families, Institute of Medicine, National Research Council *Sports-Related Concussions in Youth: Improving the Science, Changing the Culture*. at <<http://www.ncbi.nlm.nih.gov/books/NBK169016/>>. National Academies Press (US). Washington (DC). (2014).
6. Barkhoudarian, G., Hovda, D.A., Giza, C.C. The Molecular Pathophysiology of Concussive Brain Injury - an Update. *Physical Medicine and Rehabilitation Clinics of North America*. **27** (2), 373–93 (2016).
7. McCrory, P. et al. Consensus statement on concussion in sport--the 4th International Conference on Concussion in Sport held in Zurich, November 2012. *Clinical Journal of Sport Medicine*. **23** (2), 89–117 (2013).
8. Belanger, H.G., Vanderploeg, R.D., Curtiss, G., Warden, D.L. Recent neuroimaging techniques in mild traumatic brain injury. *Journal of Neuropsychiatry and Clinical Neurosciences*. **19** (1), 5–20 (2007).
9. Sours, C., Zhuo, J., Roys, S., Shanmuganathan, K., Gullapalli, R.P. Disruptions in Resting State Functional Connectivity and Cerebral Blood Flow in Mild Traumatic Brain Injury Patients. *PLoS ONE*. **10** (8), e0134019 (2015).
10. Buckley, E.M. et al. Decreased Microvascular Cerebral Blood Flow Assessed by Diffuse Correlation Spectroscopy after Repetitive Concussions in Mice. *Journal of Cerebral Blood Flow & Metabolism*. **35** (12), 1995–2000 (2015).
11. Sankar, S.B. et al. Low cerebral blood flow is a non-invasive biomarker of neuroinflammation after repetitive mild traumatic brain injury. *Neurobiology of Disease*. **124**, 544–554 (2019).
12. Vagnozzi, R. et al. Temporal window of metabolic brain vulnerability to concussions: mitochondrial-related impairment--part I. *Neurosurgery*. **61**, 379–88; discussion 388-9 (2007).
13. Longhi, L. et al. Temporal window of vulnerability to repetitive experimental concussive brain injury. *Neurosurgery*. **56**, 364–74 (2005).
14. Fujita, M., Wei, E.P., Povlishock, J.T. Intensity- and interval-specific repetitive traumatic brain injury can evoke both axonal and microvascular damage. *Journal of Neurotrauma*. **29**, 2172–80 (2012).

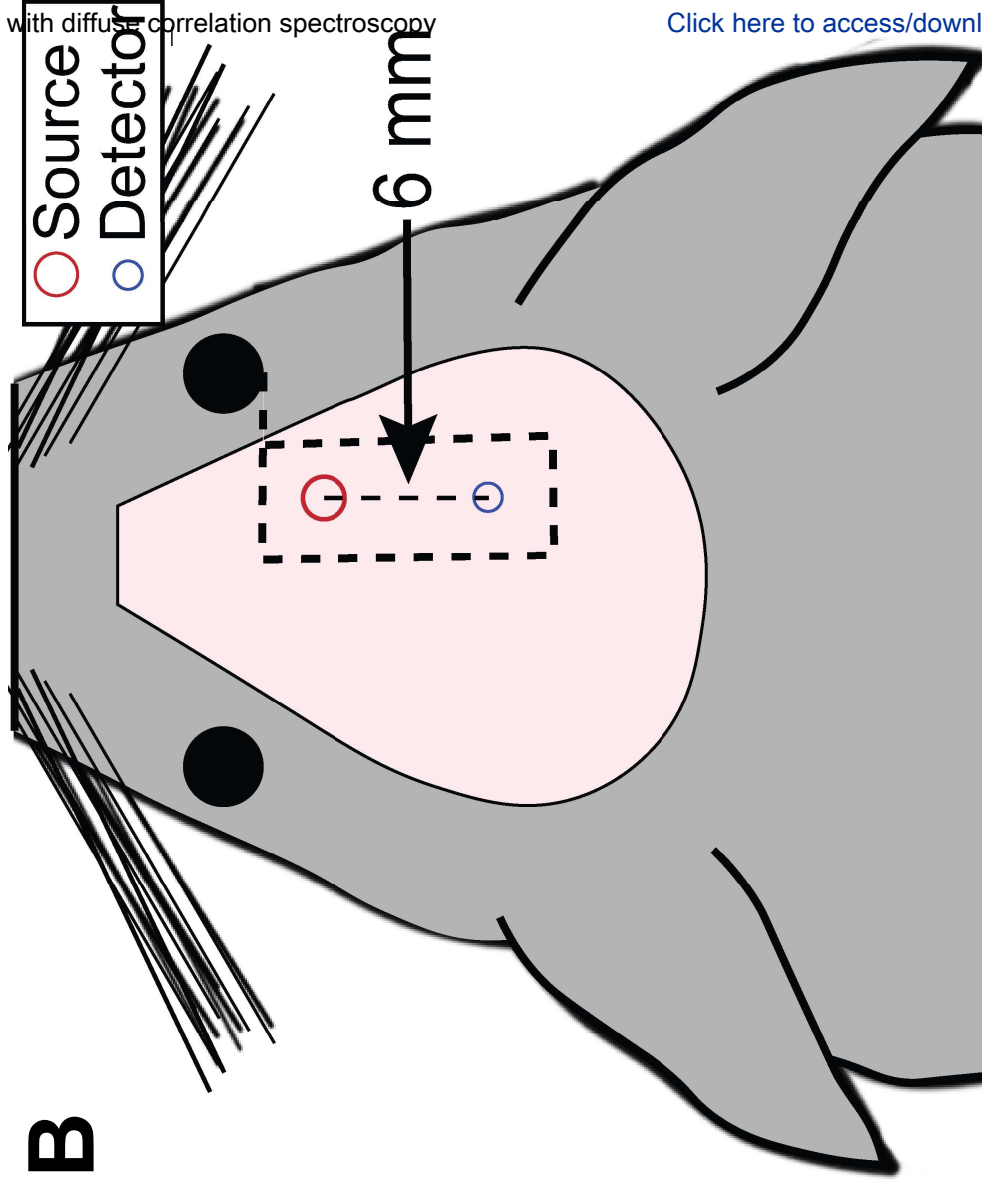
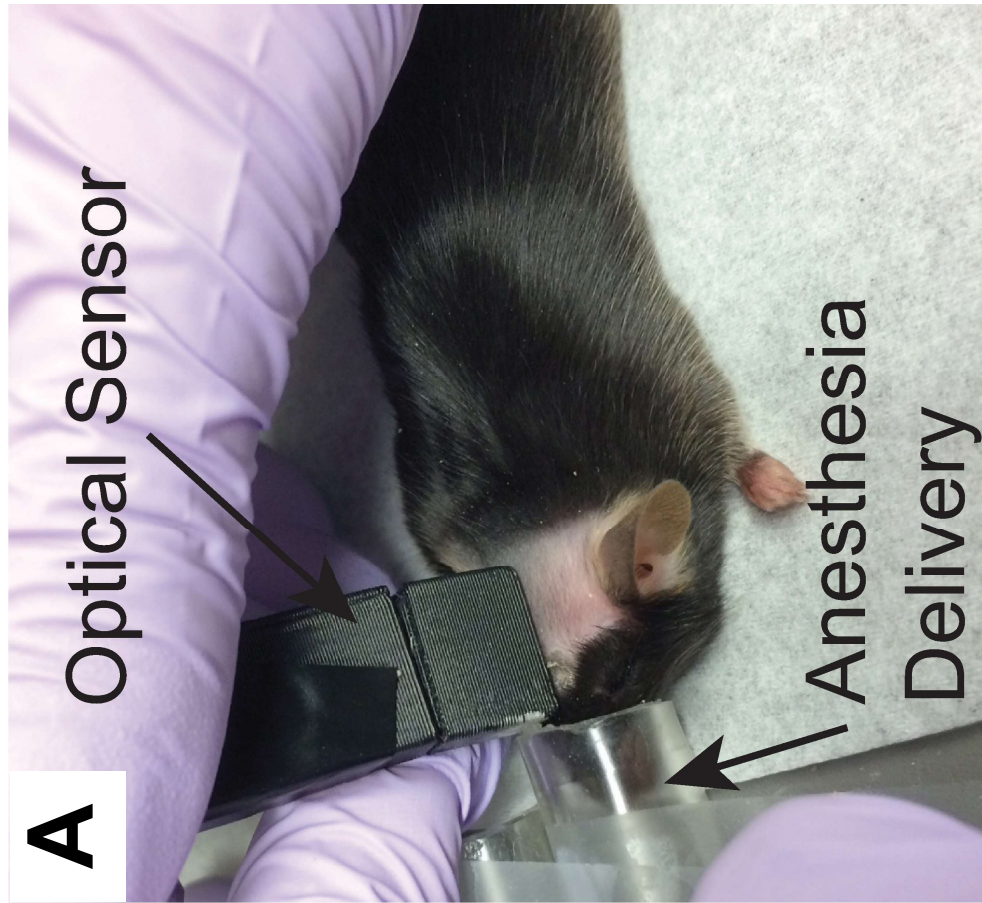
15. Angoa-Perez, M. et al. Animal models of sports-related head injury: bridging the gap between preclinical research and clinical reality. *Journal of Neurochemistry*. **129**, 916–31 (2014).
16. Prins, M.L., Hales, A., Reger, M., Giza, C.C., Hovda, D.A. Repeat traumatic brain injury in the juvenile rat is associated with increased axonal injury and cognitive impairments. *Developmental Neuroscience*. **32**, 510–8 (2010).
17. Viano, D.C., Hamberger, A., Bolouri, H., Saljo, A. Concussion in professional football: animal model of brain injury--part 15. *Neurosurgery*. **64**, 1162–73; discussion 1173 (2009).
18. Kane, M.J. et al. A mouse model of human repetitive mild traumatic brain injury. *Journal of Neuroscience Methods*. **203**, 41–9 (2012).
19. Meehan, W.P., Zhang, J., Mannix, R., Whalen, M.J. Increasing Recovery Time Between Injuries Improves Cognitive Outcome After Repetitive Mild Concussive Brain Injuries in Mice: *Neurosurgery*. **71** (4), 885–892 (2012).
20. Durduran, T., Yodh, A.G. Diffuse correlation spectroscopy for non-invasive, micro-vascular cerebral blood flow measurement. *NeuroImage*. **85**, 51–63 (2014).
21. Sathialingam, E. et al. Small separation diffuse correlation spectroscopy for measurement of cerebral blood flow in rodents. *Biomedical Optics Express*. **9** (11), 5719 (2018).
22. Lee, S.Y. et al. Noninvasive optical assessment of resting-state cerebral blood flow in children with sickle cell disease. *Neurophotonics*. **6** (03), 1 (2019).
23. Wang, H., Liu, Q., Tu, Y. Interpretation of partial least-squares regression models with VARIMAX rotation. *Partial Least Squares*. **48** (1), 207–219 (2005).
24. Eriksson, L., Byrne, T., Johansson, E., Trygg, J., Vikström, C. *Multi- and Megavariable Data Analysis Basic Principles and Applications*. Umetrics Academy. (2013).
25. Conzen, P.F. et al. Systemic and regional hemodynamics of isoflurane and sevoflurane in rats. *Anesthesia and Analgesia*. **74** (1), 79–88 (1992).
26. Durduran, T., Choe, R., Baker, W.B., Yodh, A.G. Diffuse optics for tissue monitoring and tomography. *Reports on Progress in Physics*. **73** (7), 076701 (2010).
27. Lee, S.Y. et al. Small separation frequency-domain near-infrared spectroscopy for the recovery of tissue optical properties at millimeter depths. *Biomedical Optics Express*. **10** (10), 5362–5377 (2019).
28. Bertrand, F., Maumy-Bertrand, M. *plsRglm: Partial Least Squares Regression for Generalized Linear Models*. at <<https://CRAN.R-project.org/package=plsRglm>>. (2019).
29. White, B.R., Bauer, A.Q., Snyder, A.Z., Schlaggar, B.L., Lee, J.M., Culver, J.P. Imaging of functional connectivity in the mouse brain. *PLoS One*. **6**, e16322 (2011).
30. Buckley, E.M., Parthasarathy, A.B., Grant, P.E., Yodh, A.G., Franceschini, M.A. Diffuse correlation spectroscopy for measurement of cerebral blood flow: future prospects. *Neurophotonics*. **1** (1), 011009 (2014).
31. Tate, J., Ward, G. Interferences in immunoassay. *The Clinical Biochemist. Reviews*. **25** (2), 105–120 (2004).
32. Staples, E., Ingram, R.J.M., Atherton, J.C., Robinson, K. Optimising the quantification of cytokines present at low concentrations in small human mucosal tissue samples using Luminex assays. *Journal of Immunological Methods*. **394** (1–2), 1–9 (2013).
33. Gierut, J.J. et al. Network-level effects of kinase inhibitors modulate TNF- α -induced apoptosis in the intestinal epithelium. *Science Signaling*. **8** (407), ra129 (2015).

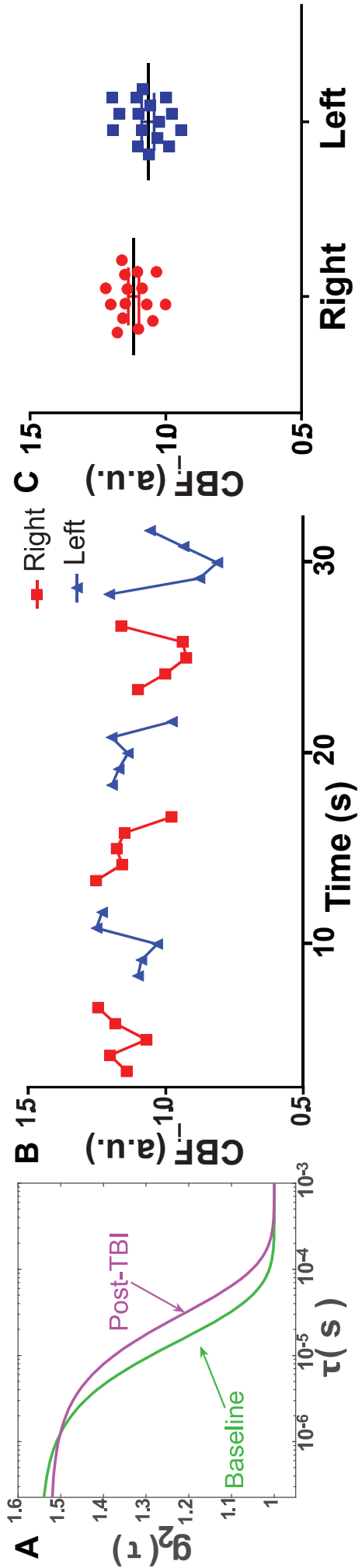
Figure 1, Typical Workflow

[Click here to access/download;Figure;Figure_1.pdf](#) 









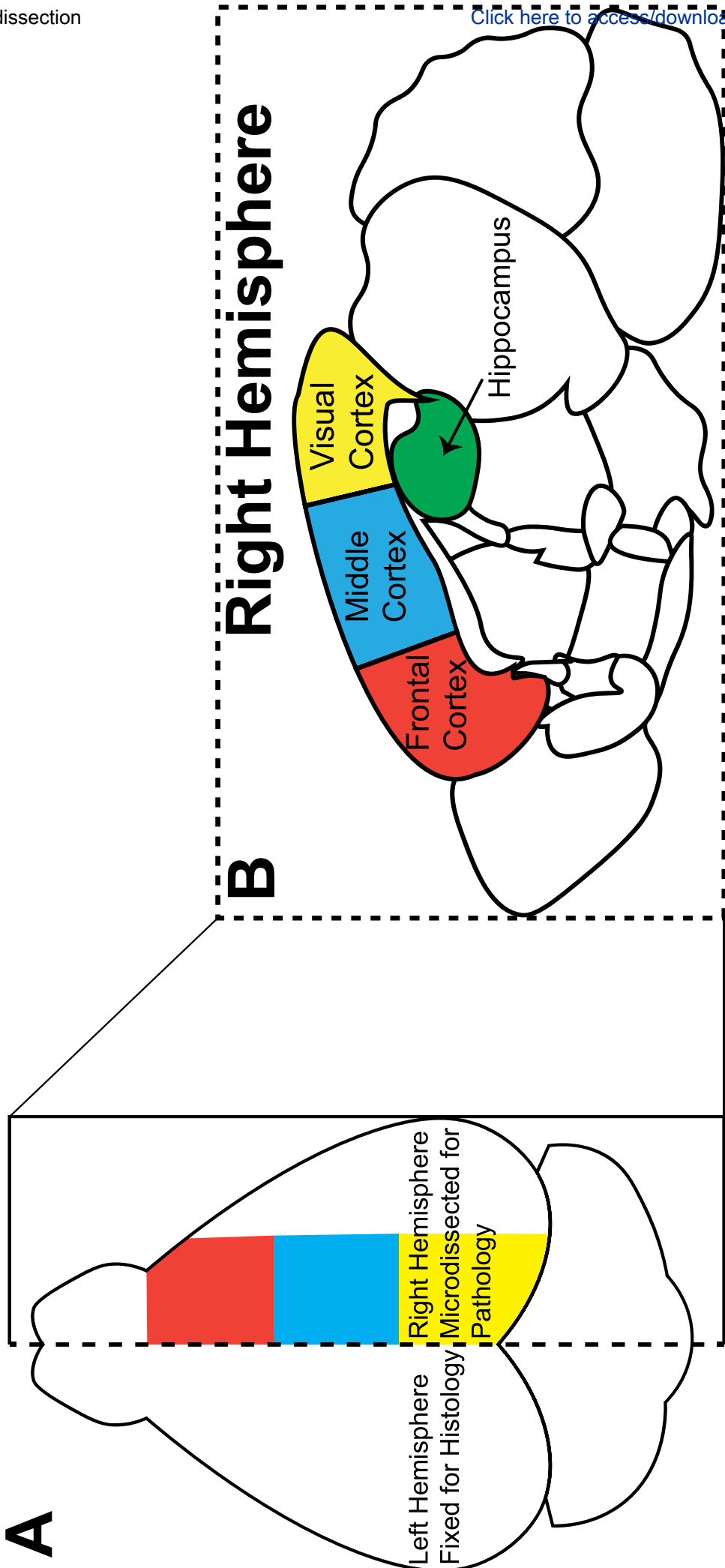
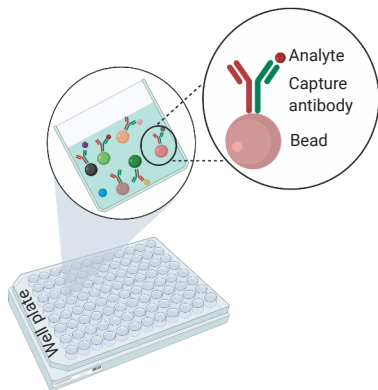


Figure 6, Illustration of Luminex
Procedure

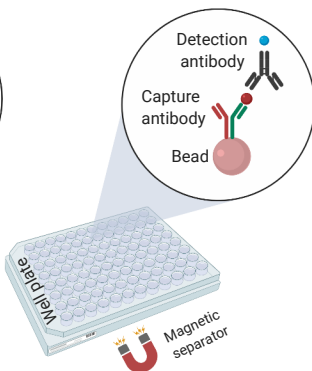
[Click here to
access/download:Figure;Figure_6.p](#)



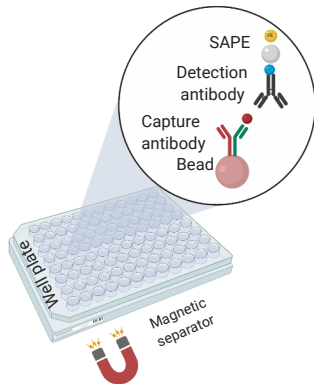
A Step 1 (Day 1)



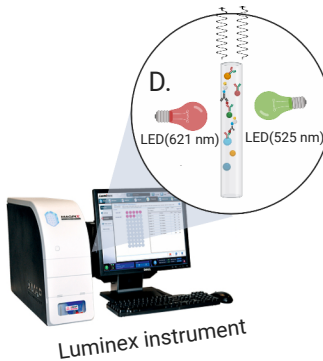
B Step 2 (Day 2)



C Step 3 (Day 2)



D Step 4 (Day 2)



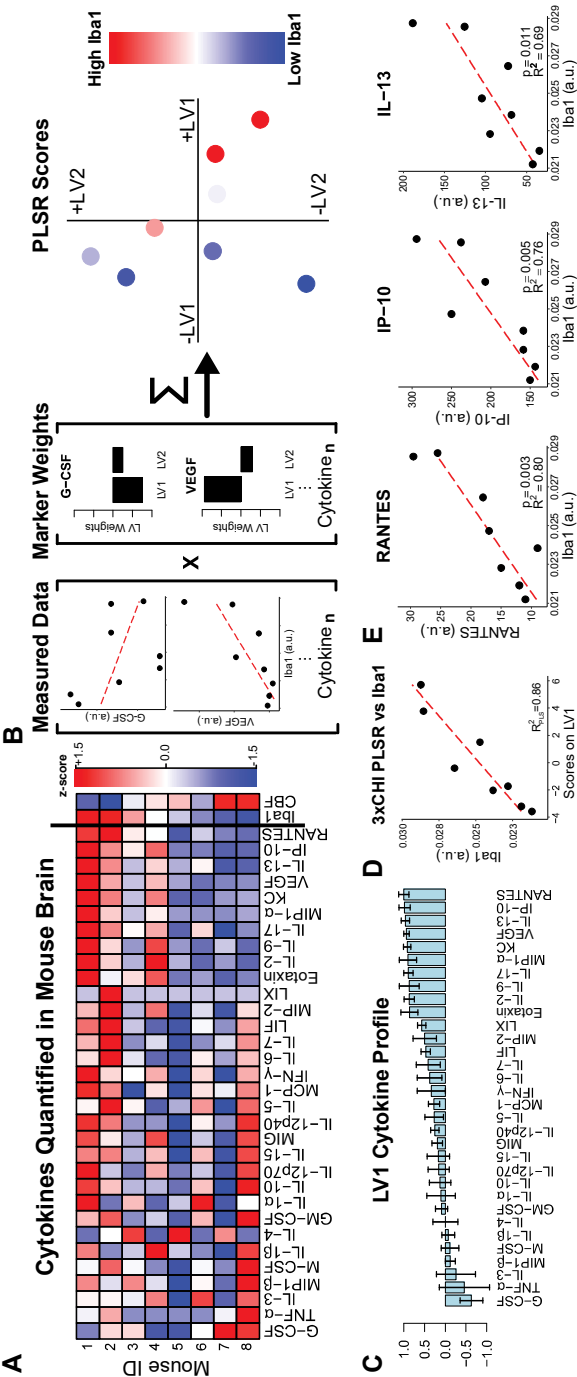
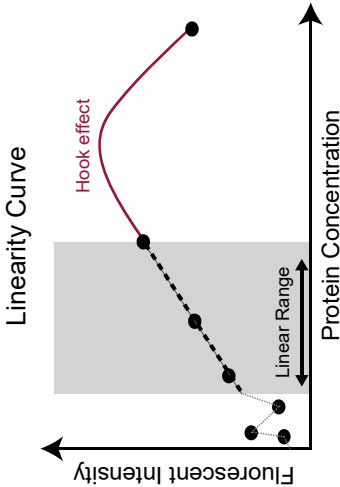


Figure 8, Illustration of sample dilution curve to identify the linear range



Name of Material/ Equipment

Adjustable pipettes
Aluminum foil
Bio-Plex cell lysis kit
BRAND BRANDplates pureGrade Microplates, Nonsterile
Complete mini protease inhibitor tablet
Depilatory cream
DiH₂O
Handheld magnetic separator block for 96 well flat bottom plates
Hardware Autocorrelator Board
Isoflurane 250 mL
Kimwipe (11.2 x 21.3 cm)
Laboratory vortex mixer
LabView
Luminex 200, HTS, FLEXMAP 3D, or MAGPIX with xPONENT software
Luminex Drive Fluid
Luminex sheath fluid
MILLIPLEX MAP Mouse Cytokine/Chemokine Magnetic Bead Panel - Premixed 32 Plex - Immunology Mul
MILLIPLEX MAPK/SAPK Signaling 10-Plex Kit-Cell Signaling Multiplex Assay
Mini LabRoller rotator
Phenylmethanesulfonyl fluoride
Phosphate-buffered Saline (PBS)
Plate Sealer
Polypropylene microfuge tubes
Mini LabRoller
Reagent Reservoirs
R Programming Language
RStudio
Sonicator
Titer plate shaker
Tween20
1 m acrylic guide tube
4 photon counting avalanche photodiode
400 um multimode source fiber
54 g bolt
780 nm single mode detector fiber
852 nm long-coherence length laser

Company**Catalog Number**

VWR	89107-726
C Bio-Rad	171304012
BrandTech	781602 96
Sigma-Aldrich	11836153001
Amazon	Nair
VWR	VWRL0200-1000
Millipore Sigma Catalogue	40-285
www.correlator.com	Flex05-8ch
MED-VET INTERNATIONAL	RXISO-250
VWR	21905-026
VWR	10153-838
National Instruments	LabVIEW
Luminex Corporation	
Luminex	MPXDF-4PK
EMD Millipore	SHEATHFLUID
Millipore Sigma	MCYTMAG-70K-PX32
Millipore Sigma	48-660MAG
VWR	10136-084
Sigma-Aldrich	P7626-1G
VWR	97064-158
VWR	82050-992
VWR	20901-547
Millipore Sigma	Z674591
VWR	89094-668
 www.rstudio.com	
VWR	12620-926
Sigma-Aldrich	P9416-50ML
McMaster-Carr	49035K85
Perkin-Elmer	SPCM-AQ4C-IO
Thorlabs Inc.	FT-400-EMT
Ace Hardware	
Thorlabs Inc.	780HP
TOPTICA Photonics	iBeam smart

Comments/Description

any adjustable pipette

0.95 cm basic body diameter, 2 cm head diameter, 10.2 cm length

5/10/2020

Journal of Visualized Experiments Editorial Office
1 Alewife Center, Suite 200
Cambridge, MA 02140 USA

Re: Resubmission of revised manuscript JoVE61504, entitled "*Systems analysis of the neuroinflammatory and hemodynamic response to traumatic brain injury.*"

Dear Dr. DSouza

We have revised our manuscript entitled "*Systems analysis of the neuroinflammatory and hemodynamic response to traumatic brain injury,*" and we are now resubmitting it for publication in *Journal of Visualized Experiments*. We thank you and the reviewers for the careful examination of our manuscript. We greatly appreciate the feedback and were glad to see that our work was appreciated by both reviewers, with reviewer #1 recognizing that "the description of the methods and analysis pipeline (including critical controls) is excellent and it provides a step-by-step approach for the reader."

Below we address questions and comments raised by both reviewers. In each response, we copy the original comment (black), provide a response (red), and then indicate text changes (if any) made to accommodate the comment. In regards to reviewer #2's comment regarding the scope of the manuscript, we have discussed this issue with Claudia Espinosa-Garcia, Guest Editor, and she determined that the current scope is well-aligned with the theme of this special issue and should remain as is. Please feel free to contact us with any further questions. We hope you find that the manuscript in its revised form is now suitable for publication.

Sincerely,



Erin M. Buckley, Ph.D.
Assistant Professor
Wallace H. Coulter Department of Biomedical Engineering, Georgia Institute of Technology and Emory University
Department of Pediatrics, Emory University
Suite E100, Room E106
1760 Haygood Dr NE
Atlanta, GA 30322

Reviewer 1

“This is an excellent JoVE paper. I congratulate the authors for providing clear protocols that detail the use of system analysis approaches to analyze neuroinflammatory and hemodynamic responses after mild TBI. The introduction and methods are beautifully written and are very clear. The protocols are detailed, yet concise, and this is very helpful for the reader[...]Again, the description of the methods and analysis pipeline (including critical controls) is excellent and it provides a step-by-step approach for the reader. The authors also provide a nice discussion section that includes strengths and limitations of the techniques/analysis platforms.”

Comment 1: Line 144. The authors should cite their study using the repeated mTBI model that results in long-term impairments in cognitive function.

Response: This reference is “Increasing Recovery Time Between Injuries Improves Cognitive Outcome After Repetitive Mild Concussive Brain Injuries in Mice”, Meehan 2012. We include this reference on Line 107 after we stated that “Key features of this model include[...]persistent (up to 1 year) cognitive deficits that emerge only after multiple hits[Meehan 2012].”

Comment 2: Fig 2. The authors should consider adding representative righting reflex data for mice following Sham and mTBI surgery as a reference data set for the TBI model.

Response: We added a supplemental table containing a representative data set.

Reviewer 2

Major issues:

Comment 1: I hope the authors will considering dividing this paper into multiple papers.

Response: We appreciate the Reviewer’s comment and have extensively discussed this very point amongst ourselves and with Claudia Espinosa-Garcia, Guest Editor of special issue “..”. Ultimately we concluded the unique aspect of our work is the integration of multiple experimental techniques, this integration gives us the capacity to investigate to disease mechanisms and as such we felt it necessary to maintain the current scope of the manuscript.

Editorial Comments

Comment 1: The JoVE protocol should be almost entirely composed of numbered short steps (2-3 related actions each) written in the imperative voice/tense (as if you are telling someone how to do the technique, i.e. "Do this", "Measure that" etc.). Any text that cannot be written in the imperative tense may be added as a brief “Note” at the end of the step (please limit notes).

1) Long descriptive sections of the protocol such as on lines 147-164, 248-262 should be made into steps/notes (limit 1 note per step) or can be moved to Representative Results or Discussion. The JoVE protocol should be a set of instructions rather a report of a study. Any reporting should be moved into the representative results.

Response: This protocol effectively covers the unique integration of four experimental procedures. We have therefore included a necessary introductory paragraph for each procedure section to aid in reader

comprehension. This text would not be appropriate for Representative Results. We would be happy to work with you to determine a better placement for this text, but as of now we feel this is the most appropriate location to aid in reader comprehension.

Comment 2: Please note that your protocol will be used to generate the script for the video, and must contain everything that you would like shown in the video. **Please add more specific details (e.g. button clicks for software actions, numerical values for settings, etc) to your protocol steps.** There should be enough detail in each step to supplement the actions seen in the video so that viewers can easily replicate the protocol.

Response: Thank you for the suggestion. We now add specific details for button clicks and software actions in RStudio to execute the PLSR analysis. The accompanying code is sectioned according to steps in the protocol. Steps were added to download all relevant programs and R packages, enabling easy replication of the protocol.

Text change: Sections 4.1 to 4.3

Comment 3: Please adjust the numbering of your protocol section to follow JoVE's instructions for authors, 1. should be followed by 1.1. and then 1.1.1. if necessary and all steps should be lined up at the left margin with no indentations. There must also be a one-line space between each protocol step.

Response: Thank you for clarifying that this type of numbering is necessary, we adjusted the numbering of our protocol accordingly.

Comment 4: After you have made all of the recommended changes to your protocol (listed above), please re-evaluate the length of your protocol section. There is a 10-page limit for the protocol text, and a 3- page limit for filmable content. If your protocol is longer than 3 pages, please highlight ~2.5 pages or less of text (which includes headings and spaces) in yellow, to identify which steps should be visualized to tell the most cohesive story of your protocol steps.

- 1) The highlighting must include all relevant details that are required to perform the step. For example, if step 2.5 is highlighted for filming and the details of how to perform the step are given in steps 2.5.1 and 2.5.2, then the sub-steps where the details are provided must be included in the highlighting.
- 2) The highlighted steps should form a cohesive narrative, that is, there must be a logical flow from one highlighted step to the next.
- 3) Please highlight complete sentences (not parts of sentences). Include sub-headings and spaces when calculating the final highlighted length.
- 4) Notes cannot be filmed and should be excluded from highlighting.

Response: We confirmed that the protocol is less than 10 pages and we have highlighted ~2.5 pages for filming a cohesive narrative.

Comment 5: JoVE articles are focused on the methods and the protocol, thus the discussion should be similarly focused. Please ensure that the discussion covers the following in detail and in paragraph form (3-6 paragraphs): 1) modifications and troubleshooting, 2) limitations of the technique, 3) significance with respect to existing methods, 4) future applications and 5) critical steps within the protocol.

Response: We have ensured that we thoroughly address all of these concerns in our discussion.

Comment 6: Fig 6 is called out before 5. Please re-order figures.

Response: Thank you for bringing this to our attention, we re-ordered figures 5 and 6.

Comment 7: JoVE is unable to publish manuscripts containing commercial sounding language, including trademark or registered trademark symbols (TM/R) and the mention of company brand names before an instrument or reagent. Examples of commercial sounding language in your manuscript are McMaster-Carr, Kimwipe, Kimberly-Clark, SPCM-AQ4C-IO, Perkin-Elmer, (Flex05-8ch, www.correlator.com, cOmplete™, etc.

1) Please use MS Word's find function (Ctrl+F), to locate and replace all commercial sounding language in your manuscript with generic names that are not company-specific. All commercial products should be sufficiently referenced in the table of materials/reagents. You may use the generic term followed by "(see table of materials)" to draw the readers' attention to specific commercial names.

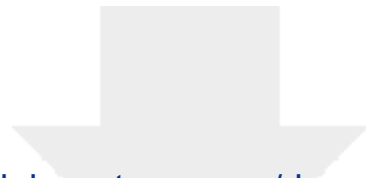
Response: Thank you, we removed all of the commercial language from our manuscript except Luminex, which is a distinct type of immunoassay.

Comment 8: Please sort Table of Materials in alphabetical order.

Response: Thank you for the comment. We have made this correction.

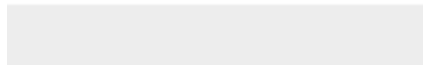
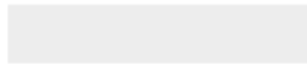
Loss of Consciousness (LoC) over 5 Hits						
Group	Mouse ID	Hit 1 LoC (s)	Hit 2 LoC (s)	Hit 3 LoC (s)	Hit 4 LoC (s)	Hit 5 LoC (s)
Injured	Mouse 1	66	78	79	98	110
	Mouse 2	54	72	63	82	80
	Mouse 3	60	84	99	110	114
Sham	Mouse 4	62	53	58	60	55
	Mouse 5	49	57	53	48	58
	Mouse 6	50	47	57	60	50

Supplemental Table 1. Representative loss of consciousness data for 6 mice (3 injured, 3 sham) over the course of 5 injuries, spaced once daily. Data represents time in seconds for each mouse to regain righting reflex after removal from anesthesia. Injured mice were subject to our weight-drop model of mild traumatic brain injury (**Section 1.**) while sham mice were simply exposed to anesthesia for the same duration. Sham mice show no increase in loss of consciousness with once-daily exposure to anesthesia. Injured mice show increases in loss of consciousness with each successive injury – however, to date we have not seen loss of consciousness correlate with functional outcome.



[Click here to access/download](#)

Supplemental Coding Files
PLSR_Sample_Code_AFP.pdf





Click here to access/download
Supplemental Coding Files
MyData.xls